Supporting information

How Do Surface Defects Change Local Wettability of Hydrophilic ZnS Surface? Insights on Sphalerite Flotation from DFT Calculations

Abolfazl Alizadeh Sahraei, Faïçal Larachi*

Department of Chemical Engineering, Université Laval, 1065 Avenue de la Médecine, Québec, Québec G1V 0A6, Canada

corresponding author:

Email: faical.larachi@gch.ulaval.ca (Faïçal Larachi)

Number page: 10

Number of Figures: 4

Number of Table: 3

Monte Carlo initialization: output data

Monte Carlo algorithm combined with simulated annealing was chosen to statistically search for the lowest energy configurations of water molecules on the ZnS slab. For each cases, we applied the searching algorithm for ten cycles with 100000 steps per each cycle. The Monte Carlo outputs and the suggested configurations for the adsorption of 48 water molecules on the ZnS with a single sulfur deficiency, as an example, are respectively provided in Table S1 and Figure S1.

Table S1: Output results obtained by the Monte Carlo algorithm for the adsorption of 48 water molecules on the sulfur-deficient ZnS slab

Structures	Total energy (kcal/mol)	Adsorption energy (kcal/mol)	dEad/dNi
$\mathbf{I_S}$	-112.586	-134.157	-2.92
$\mathbf{II_S}$	-112.082	-133.653	-2.91
$\mathbf{III_S}$	-111.549	-133.120	-2.97
$\mathbf{IV_S}$	-110.960	-132.531	-2.78
$\mathbf{V_S}$	-110.332	-131.903	-2.88
$\mathbf{VI_S}$	-110.051	-131.623	-2.74
$\mathbf{VII_S}$	-109.812	-131.383	-2.86
$\mathbf{VIII_S}$	-109.104	-130.675	-2.33
$\mathbf{XI_S}$	-108.871	-130.442	-3.06
$\mathbf{X_S}$	-108.652	-130.224	-2.96

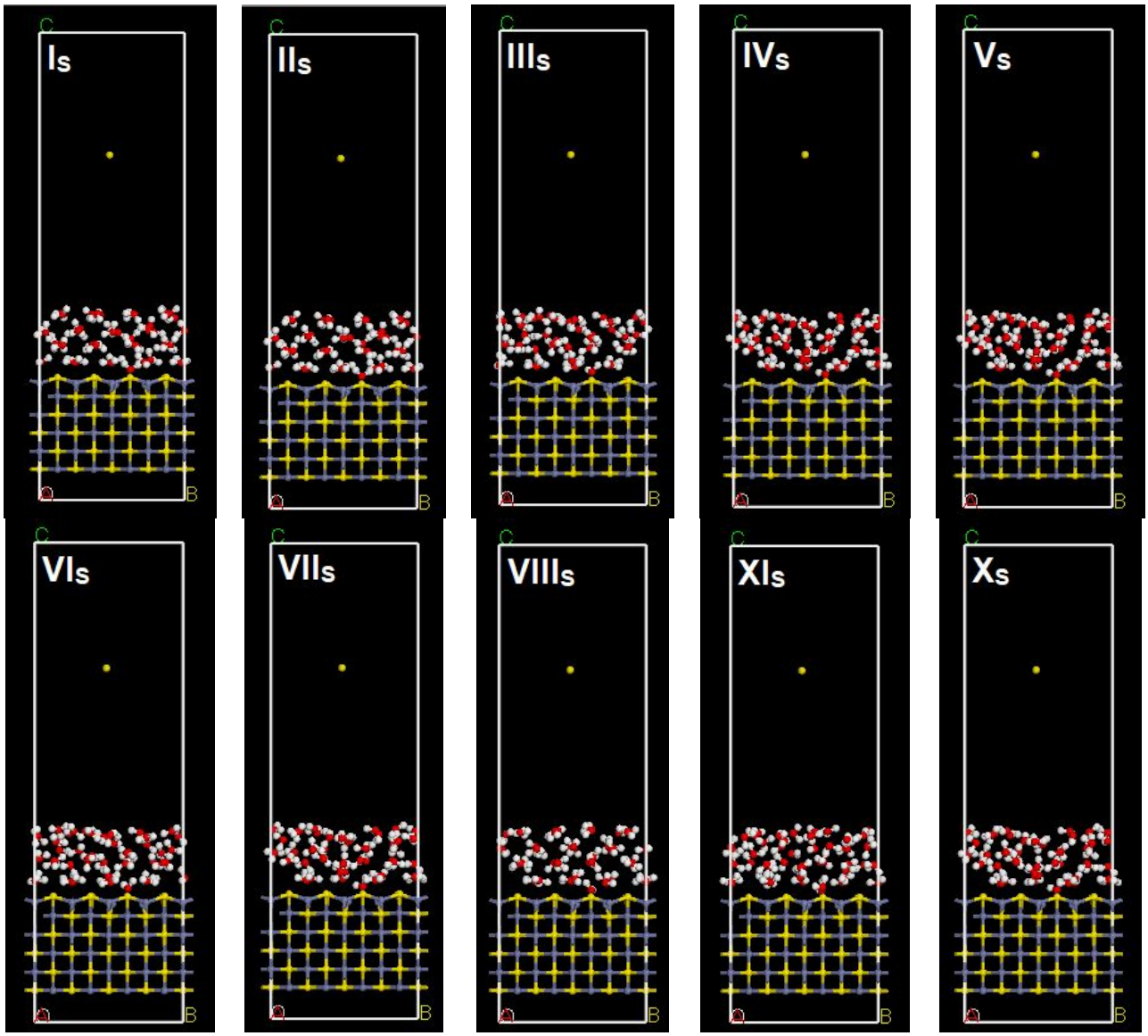

Figure S1: Output adsorption configurations of 48 water molecules on the sulfur deficient ZnS slab obtained by the Monte Carlo algorithm related to the data in **Table S1.**

Adsorption of monolayer water molecules

To better understand how the excess number of water changes the water-surface interactions, we next increased the number of water molecules up to a monolayer to slightly involve the competition of both water-surface and water-water interactions in the simulation. In order to interpret the adsorption cases conveniently, fixed numbers of H_2O molecules were added on top of the slabs, considering two different scenarios for the population of the water molecules to form a monolayer. A monolayer was defined as 1) one water molecule for every surface cation site located on the surface upper hill, or 2) one water molecule for every cation and anion site on the surface upper hill to build a saturated adsorption model. Based on the definitions, 12 and 24 water molecules were initially adsorbed on the ZnS surface following the first and second scenarios.

Figure S2 displays the most energetically favorable configurations for ZnS (110) surface in different environments with 12 adsorbed water molecules. The details of the interactions, categorized as surface-water and water-water interactions, are summarized in Table S2. Based on the results obtained, the interaction energy per water molecule in the monolayer is less than those of the isolated water molecule. However, the trend is still the same, in which the II_S model is the most hydrophobic surface, and the $V_{Zn(u)S(d)}$ shows the most hydrophilic nature. Apart from the new adsorption pattern for the monolayer adsorption, the difference in the value of the interaction energy can be attributed to hydrogens' competing interest to bond with the sulfur atom, which itself would contribute to weakening the water adsorption.[1] For the case of the II_S complex, minimum numbers of covalent and hydrogen bonds were formed between the surface and water molecules, as given in Table S2. Compared to the adsorption of an isolated water, the greatest difference (~155%) in the value of the interaction energy was observed for the $V_{Zn(u)S(d)}$ surface. By excessing the number of water molecules, no dissociation reaction was observed on the $V_{Zn(u)S(d)}$ surface, as seen in Figure S2, which causes a dramatic increase in the interaction energy value. The optimized water monolayers in Figure S2 shows an almost ordered structure except for the II_S sample, in which a small disordered pattern can be recognized by observing its cross-view image. After the monolayer water adsorption, the majority of the metal atoms on the surface upper hill moves closer to the bulklike positions since their coordination number has increased from 3-fold to 4-fold.

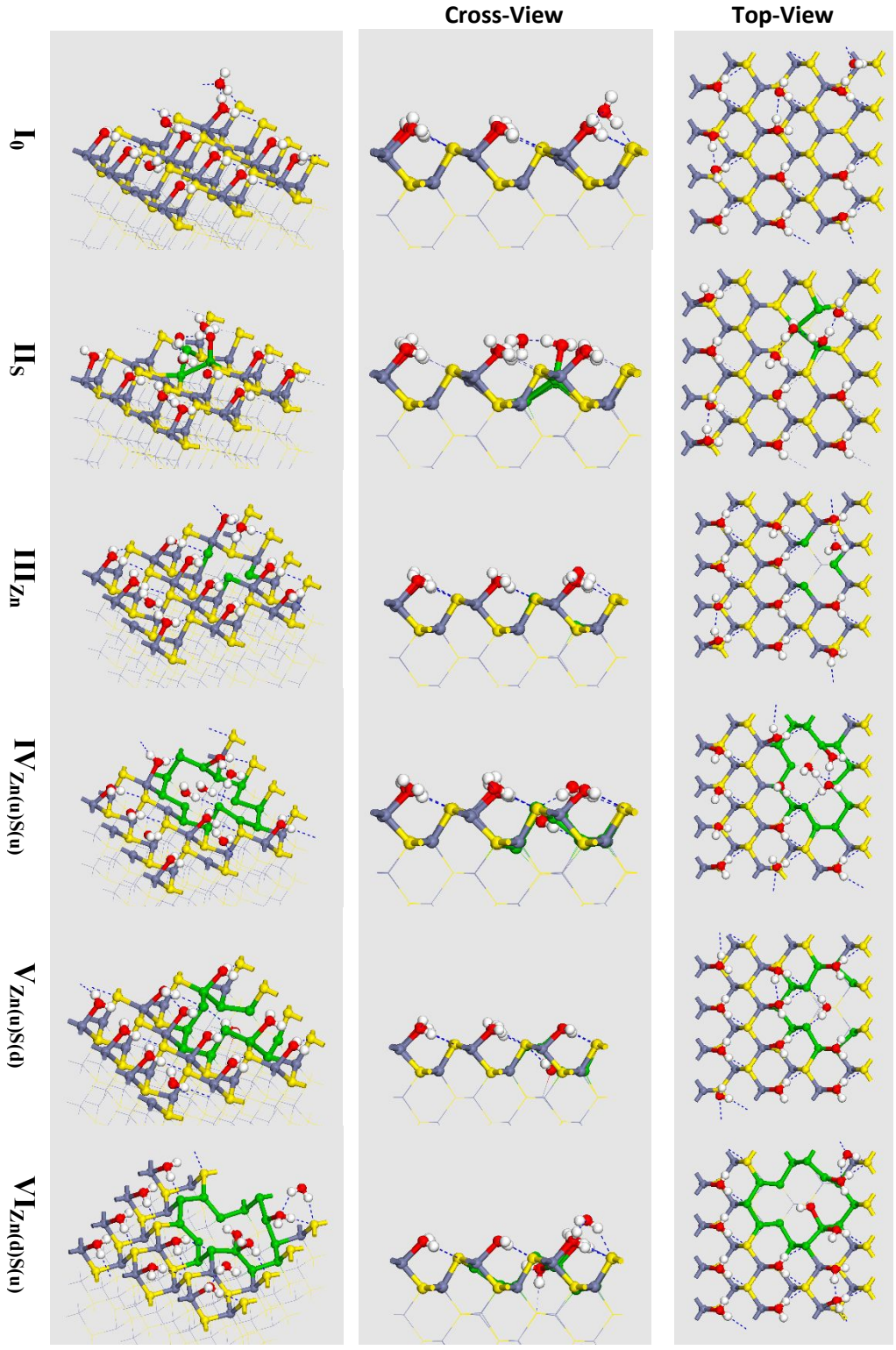

Figure S2. The most energetically favorable configurations for the adsorption of 12 water molecules on the defect-free (I_0), sulfur-deficient (II_S), zinc-deficient (III_{Zn}), and congruent neighboring deficient ($IV_{Zn(u)S(u)}$, $V_{Zn(u)S(u\backslash d)}$, and $VI_{Zn(d)S(u)}$) ZnS (110) surfaces. The blue dashed line represents the hydrogen bond. The atoms on the edge of the vacancy colored as green. (Zn ≡ Purple, S ≡ Yellow, N ≡ Blue, O ≡ Red, C ≡ Gray, H ≡ White).

Table S2. Characterization of the covalent and hydrogen bonding and the interaction energy for the complexes with 12 water molecules on the ZnS (110) surface with different vacancy types related to the most energetically favorable adsorption modes shown in **Figure S2**. The values in parenthesis are the average.

Sample	Surface-Water Interactions					Water-Water Interactions			E_{int} (kcal/mol)
	# *covalent bond*	*d (Zn-O) (Å)*	# *H-bond*	*d (H···S) (Å)*	*O-H···S (deg)*	# *H-bond*	*d (H···S) (Å)*	*O-H···O (deg)*	
$\mathbf{I_0}$	9	2.13-2.21 (**2.19**)	14	2.03-2.63 (**2.38**)	136-173.6 (**161.5**)	4	1.74-2.36 (**1.96**)	145-172.8 (**160.7**)	-21.28
$\mathbf{II_S}$	7	2.12-2.24 (**2.20**)	13	2.24-2.60 (**2.40**)	141.9-176.9 (**161.8**)	5	1.69-2.65 (**2.00**)	114.6-164.6 (**150.2**)	-19.68
$\mathbf{III_{Zn}}$	10	2.16-2.23 (**2.19**)	14	2.18-2.58 (**2.40**)	134.3-179.2 (**160.8**)	3	1.61-2.37 (**1.99**)	142-166.5 (**153.2**)	-21.87
$\mathbf{IV_{Zn(u)S(u)}}$	8	2.07-2.23 (**2.18**)	14	2.19-2.62 (**2.36**)	136.9-173.4 (**163.5**)	3	1.68-2.56 (**2.21**)	139.1-167.3 (**150.1**)	-24.28
$\mathbf{V_{Zn(u)S(d)}}$	11	2.14-2.23 (**2.19**)	17	2.21-2.63 (**2.40**)	138.9-174.7 (**160.7**)	2	2.31-2.40 (**2.35**)	130.8-154.4 (**142.6**)	-26.43
$\mathbf{VI_{Zn(d)S(u)}}$	11	2.19-2.21 (**2.20**)	14	2.13-2.63 (**2.36**)	139-178.4 (**164.4**)	3	1.64-2.26 (**1.95**)	131.3-168.7 (**151.5**)	-23.00

The most stable structures correspond to the adsorption of 24 water molecules on the ZnS (110) surface, along with their characterization details, are respectively provided in Figure S3 and Table S3. With the 24 water molecules on the surface, the interaction energy per one water molecule increased; however, the trend was still preserved. Compared with the adsorption of 12 water molecules, the average lengths of the *Zn-O* and *H···S* in the 24 water-ZnS complexes have been shrunk except for the defect-free slab. This shows that 12 water molecules are not enough to form a saturated monolayer of water on the defective surfaces. It is clearly observed in Figure S3 that the adsorption pattern of a saturated monolayer of water molecules differs from that of the isolated water. For the isolated water on the ZnS surface, both two *H* atoms of water participate in the surface-water interaction by forming two *H···S* hydrogen bonds, whereas, for the saturated monolayer water complex, only one *H* atom forms an H-bond with the *S* of the surface layer. The other *H* atom bonds to the *O*

of the nearest water molecule (i.e., *H···O* bond) to form its second H-bond. This suggests that the water molecules near the first adsorbed water layer alter the water-surface interaction. Therefore, the simplified view for the adsorption of an isolated water molecule cannot reflect the real phenomenon at the water-mineral surface interfaces in aqueous solid suspensions.

Table S3. Characterization of the covalent and hydrogen bonding and the interaction energy for the complexes with 24 water molecules on the ZnS (110) surface with different vacancy types related to the most energetically favorable adsorption modes shown in **Figure S3**. The values in parenthesis are the average.

Sample	**Surface-Water Interactions**					**Water-Water Interactions**			**E_{int} (kcal/mol)**
	# covalent bond	*d (Zn-O) (Å)*	*# H-bond*	*d (H···S) (Å)*	*O-H···S (deg)*	*# H-bond*	*d (H···S) (Å)*	*O-H···O (deg)*	
I_0	12	2.14-2.23 (**2.18**)	17	2.01-2.64 (**2.37**)	145.8-172.7 (**159.3**)	25	1.50-2.64 (**1.77**)	109.9-175.5 (**164.8**)	-12.43
II_S	9	2.05-2.22 (**2.17**)	16	2.10-2.48 (**2.31**)	146.9-176.2 (**165.1**)	27	1.57-2.48 (**1.91**)	111.9-176.5 (**153.5**)	-12.32
III_{Zn}	11	2.10-2.24 (**2.17**)	16	2.10-2.64 (**2.34**)	139.8-177.6 (**163.3**)	27	1.51-2.55 (**1.80**)	121.8-176.5 (**162.0**)	-13.08
$IV_{Zn(u)S(u)}$	10	2.07-2.24 (**2.18**)	17	2.10-2.65 (**2.34**)	146.2-174.4 (**164.6**)	26	1.51-2.21 (**1.79**)	132.7-178 (**162.1**)	-14.84
$V_{Zn(u)S(d)}$	10	2.09-2.23 (**2.14**)	21	1.97-2.53 (**2.30**)	131.5-175.6 (**162.0**)	26	1.49-2.60 (**1.90**)	106.8-176 (**155.2**)	-16.76
$VI_{Zn(d)S(u)}$	9	2.12-2.23 (**2.17**)	16	2.00-2.62 (**2.30**)	141.0-177.3 (**163.3**)	26	1.55-2.41 (**1.80**)	141.5-177.4 (**164.1**)	-14.06

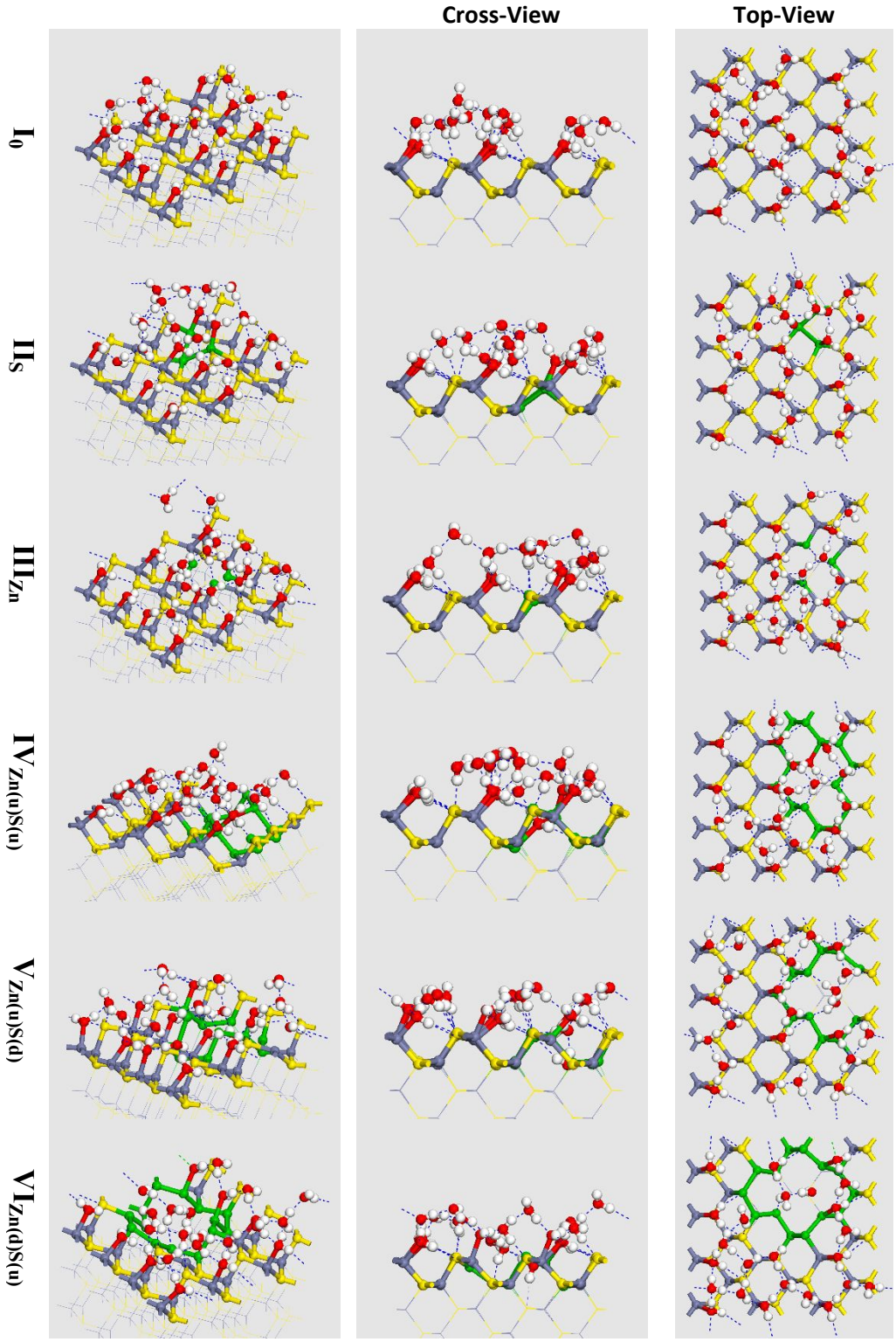

Figure S3. The most energetically favorable configurations for the adsorption of 24 water molecules on the defect-free (I_0), sulfur-deficient (II_S), zinc-deficient (III_{Zn}), and congruent neighboring deficient ($IV_{Zn(u)S(u)}$, $V_{Zn(u)S(u\backslash d)}$, and $VI_{Zn(d)S(u)}$) ZnS (110) surfaces. The blue dashed line represents the hydrogen bond. The atoms on the edge of the vacancy colored as green. (Zn ≡ Purple, S ≡ Yellow, N ≡ Blue, O ≡ Red, C ≡ Gray, H ≡ White).

Explicit vs. implicit water models

In DFT calculations, the solvation effects are used to be accounted for implicitly using different methods and whereby the conductor-like screening model (COSMO) is perhaps the most emblematic of them.[2] In the COSMO approach, for example, a solvent is approximated by a continuum dielectric constant to calculate the electrostatic interactions between molecules and the solvent. However, such implicit formulations are unable to model the surface condition upon the existence of solvent molecules. In general, for the processes in aqueous solutions, surface hydration and reconstruction are prevalent. For instance, our DFT results for the explicit water/ZnS system revealed that the sphalerite surface undergoes a reformulation in the presence of water molecules, which is expected to affect the adsorption modes of the subsequent molecule from the fluid phase.

To check the hypothesis, we re-simulated the special case of adsorption of alanine on the Zn(u)S(u) slab that we had investigated in our previous work, this time by considering the water effect using the COSMO model. We restricted our survey to the most favorable configuration, in which alanine was dissociatively adsorbed on the Zn(u)S(u) slab. The optimized configuration is shown in Figure S4. As shown in the figure, after implicitly applying the water effect, the alanine molecule dissociatively adsorbed on the surface, forming a tridentate bond with the Zn(u)S(u) surface. The adsorption mode here is the same as the one we obtained for the gas-phase adsorption;[3] however, the alanine affinity differs for the two cases. The result endorses the fact that in the case of solvated systems, it is necessary to explicitly investigate the reconstruction and reformulation of the surface before progressing to model the adsorption of solvent-laden reagents.

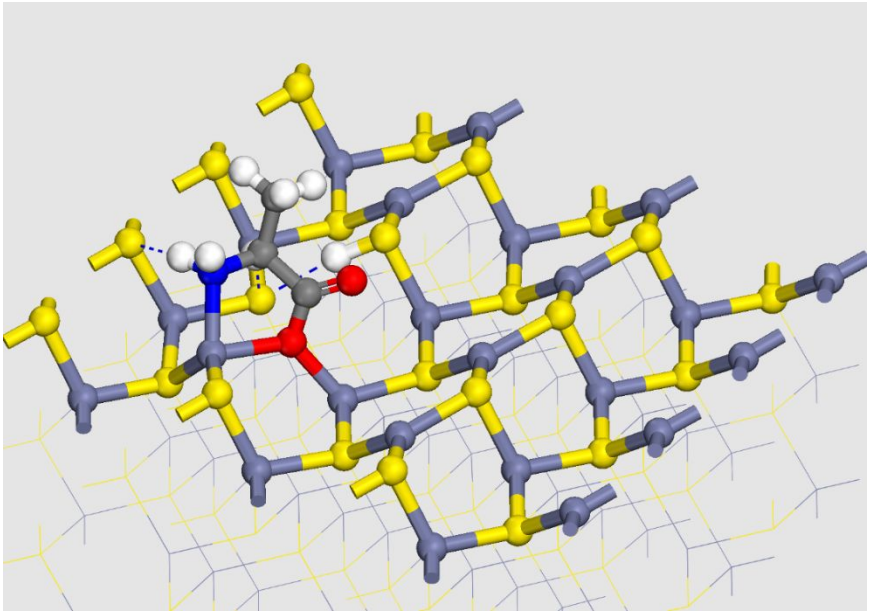

Figure S4. Optimized configurations of an alanine molecule on the Zn(u)S(u) (110) surface in the liquid-phase using the COSMO model. The "u" letter refers to the position of the vacancy on the *upper hill* of the surface layer. The blue dashed line represents the hydrogen bond. (Zn ≡ Purple, S ≡ Yellow, N ≡ Blue, O ≡ Red, C ≡ Gray, H ≡ White).

References

(1) Stirling, A.; Bernasconi, M.; Parrinello, M. Ab Initio Simulation of Water Interaction with the (100) Surface of Pyrite. *J. Chem. Phys.* **2003**, *118*, 8917-8926.
(2) Klamt, A. Conductor-Like Screening Model for Real Solvents: A New Approach to the Quantitative Calculation of Solvation Phenomena. *J. Chem. Phys.* **1995**, *99*, 2224-2235.
(3) Alizadeh Sahraei, A.; Larachi, F. Chemical Transformation and Dissociation of Amino Acids on Metal Sulfide Surface: Insights from DFT into the Effect of Surface Vacancies on Alanine-Sphalerite System. *Appl. Surf. Sci.* **2021**, *540*, 148304.